Model reduction for fluid flows in a probabilistic framework. Application to control.

L. Mathelin[1] O. Le Maître[1,2]

[1]LIMSI (Orsay)

[2]LMEE (Université d'Evry)

INRIA / IMB – March 31 - April 2, 2008

Motivations

Why should a reduced model be robust ?

- some parameters or terms of the original system are poorly known,
- to regularize a badly-conditioned model,
- to widen the range of the model validity.

Uncertainty sources

- physical properties,
- boundary / initial conditions,
- parameters of the system (*e.g.* geometry),
- ...

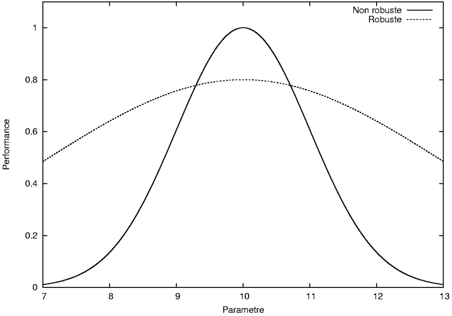

The robust control tends to guarantee a minimum level of performance with a given probability.

Cooking recipe for a robust control

Need for a reliable and fast method able to “predict” the future. Requires:

- a *light* model $\longrightarrow$ a reduced model which retains the essential dynamics and features,
- a cheap and stable time-marching scheme.

Settings of the problem at hand: 2-D flow around a circular cylinder (laminar regime)

- control intensity μ unknown a priori, $\mu \in \Omega_\mu$,
- uncertain parameters: flow Reynolds number, $Re \in \Omega_{Re}$.

$\longrightarrow$ the reduced model must remain accurate on the whole range $\Omega_\mu \otimes \Omega_{Re}$.

Cooking recipe (cont'd)

Objective function: need for a *robust* formulation of the cost function to minimize.

Robust cost function $\longrightarrow$ tries to guarantee maximum performance despite fluctuating / unknown external conditions.

$\Longrightarrow$ Investigation of the relevance and performance of this cooking recipe through the drag reduction of the 2-D flow around a circular cylinder with an uncertain Reynolds number ($\overline{Re} = 200$).

Outline

1. Physical system reduction
2. Time marching
3. Open loop robust control
4. Optimal reduction for experiments

1^{st} ingredient: robust reduced basis

Need to derive a basis truly robust w.r.t. uncertain flow parameters. Use of the Proper Orthogonal Decomposition (POD).

$$u(\boldsymbol{x}, t) = \sum_i a_i(t)\, \varphi_i(\boldsymbol{x}).$$

The reduced basis is optimal in the energy sense:

$$\varphi \setminus \ \text{arg max}_{\varphi'} \left\{ \frac{\langle |\ (u; \varphi')\ |^2 \rangle}{\|\varphi'\|^2} \right\}, \quad \varphi' \in \mathcal{L}^2([0;1]).$$

The ensemble operator is defined as

$$\langle f \rangle = \int_T \int_{\Omega_\mu} \int_{\Omega_{Re}} f(t, \mu, Re)\, p(t)\, p(\mu)\, p(Re)\, dRe\, d\mu\, dt,$$

with $p(t)$, $p(Re)$ et $p(\mu)$ the probability density function of t, Re et μ respectively.

Robust basis - POD

Assuming $p(t)$ constant and approximating the μ- et Re-integrals using cubature, it yields:

$$\langle f \rangle \simeq \int_T \sum_i^{N_q} f(t, \mu_i, Re_i)\, w_i\, dt,$$

▸ Cubature

with N_q the number of cubature points and w_i the associated weights. The POD formulation then writes:

$$\int_{T'} \sum_j^{N_q} \mathcal{R}(t, t', \mu_i, \mu_j, Re_i, Re_j)\, a(t', \mu_j, Re_j)\, w_j\, dt' = \lambda\, a(t, \mu_i, Re_i),$$

where

$$\mathcal{R}(t, t', \mu_i, \mu_j, Re_i, Re_j) = \int_{\Omega_{x'}} u(\boldsymbol{x'}, t', \mu_i, Re_i)\, u(\boldsymbol{x'}, t, \mu_j, Re_j)\, d\boldsymbol{x'},$$

and finally

$$\varphi_j(\boldsymbol{x}) = \frac{1}{\lambda_j} \int_T \sum_i^{N_q} a_j(t, \mu_i, Re_i)\, u(\boldsymbol{x}, t, \mu_i, Re_i)\, w_i\, dt.$$

$\Longrightarrow$ **Optimal basis for the energy in the $p(Re)$ and $p(\mu)$ sense.**

2-D Navier-Stokes code

Simulating the 2-D flow around a circular cylinder

- $\psi - \omega$ formulation,
- boundary conditions are imposed through an influence matrix technique,
- centered 2nd order scheme (spatial), 1st order in time. Convection terms: 4th order upwind,
- 180×180 mesh,
- solver based on a Fast Fourier Transform for the laplacian and the Poisson operator.

POD determined from 70 * ($N_q = 17$) snapshots.

Basis robustness

The reduced basis accuracy is quantified by $E_\Omega = \dfrac{\int_{\Omega_x} \left(\omega_{DNS} - \omega_{POD}\right)^2 \, dx}{\int_{\Omega_x} \omega_{DNS}^2 \, dx}$.

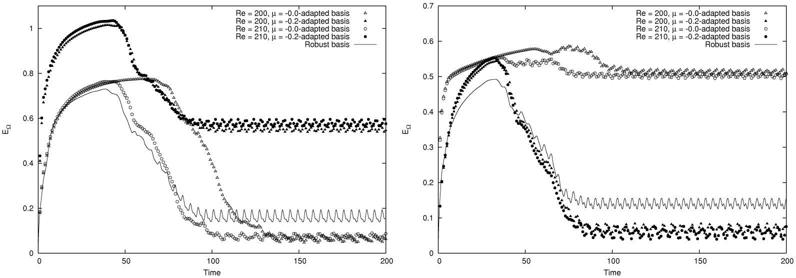

$Re = 200$ $Re = 210$

"Energy" defect of the robust reduced basis in time.

⟹ Reasonably good performance throughout the range of flow parameters.

Robust POD modes

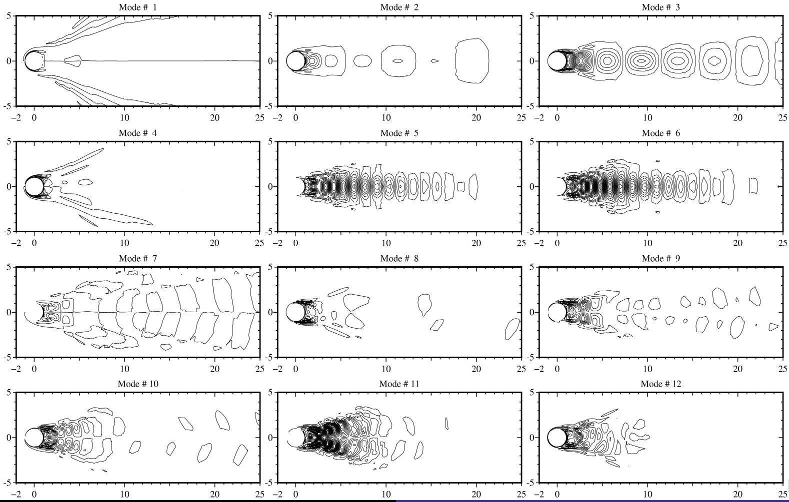

Time integration: mapping technique (MTS)

- POD $\longrightarrow$ reduction of the flow to a dynamical system Σ of low dimensionality n:
  $$u(\boldsymbol{x}, t) = \sum_i^n a_i(t)\, \varphi_i(\boldsymbol{x}),$$
- $\overline{a_i(t)} = 0$ but no further a priori information on temporal coefficients a_i of Σ $\longrightarrow$ assumed uniformly distributed on their subspace Ω_i,
- use of polynomials to get an approximation of the mapping $\mathcal{M}_T : \mathbb{R}^n \rightarrow \mathbb{R}^n$ of the coefficients over a time horizon T: $\boldsymbol{a}(t+T) = \mathcal{M}_T(\boldsymbol{a}(t))$,
- Smolyak cubature to approximate the inner products in the phase space (greedy approach suitable as well):

$$\langle f(\boldsymbol{x}, t, \boldsymbol{\xi})\, g(\boldsymbol{x}, t, \boldsymbol{\xi}) \rangle \; = \int_{\Omega_\xi} f(\boldsymbol{x}, t, \boldsymbol{\xi})\, g(\boldsymbol{x}, t, \boldsymbol{\xi})\, p(\boldsymbol{\xi})\, d\boldsymbol{\xi} \; \simeq \sum_{i=1}^{N_q} f(\boldsymbol{x}, t, \boldsymbol{\xi}_i)\, g(\boldsymbol{x}, t, \boldsymbol{\xi}_i)\, w_i$$

  $\longrightarrow$ N_q points only. Their trajectory in the phase space is to be determined using "DNS" over the time horizon T.
- Successive applications of the mapping to time integrate. Intrinsic stability even for very long time integration (several thousands of Kármán periods).

Mapping technique (MTS)

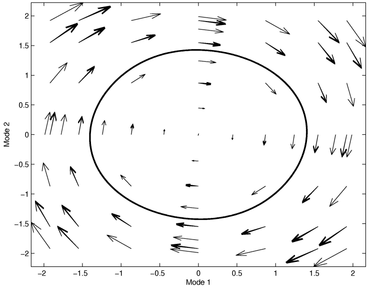

Mapping in the plane mode 1 - mode 2. The exact limit cycle (DNS) is plotted for comparison. $T = 20$, 12 POD modes.

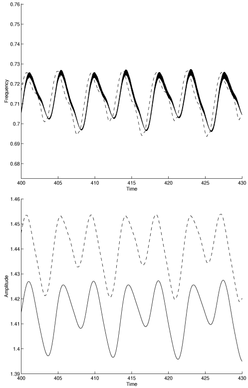

Temporal evolution of mode 2. DNS (solid line) and MTS (dotted line). Frequency (top) and amplitude (bottom).

Drag control

The control is applied with a uniform suction $\mu(t)$ throughout the surface of the porous cylinder. One minimizes the objective function using an optimal control technique based on the $\mathscr{H}_\infty$ formulation.

$$\mathscr{J} = \frac{\alpha}{2}\langle \mu; \mu \rangle + \frac{\beta}{2}\langle\langle F_D; F_D \rangle\rangle - \frac{\gamma}{2}\langle \phi; \phi \rangle,$$

where $\langle \cdot \rangle$ expresses as

$$\langle f; g \rangle = \int_{t_0}^{t_0+T_w} f(t).M_\Diamond.g^*(t)\,dt + c.c.,$$

and $\langle\langle \cdot \rangle\rangle$ as

$$\langle\langle f; g \rangle\rangle = \int_{t_0}^{t_0+T_w} \int_{\Omega_\xi} f(t,\xi).M_\Box.g^*(t,\xi)\,p(\xi)\,d\xi\,dt + c.c.,$$

Here, $M_\Diamond \equiv \mathbb{I}$, $M_\Diamond \equiv \mathbb{I}$, $\xi_i = \mathcal{N}(0,1)$.

$\longrightarrow$ Use of a stochastic code to get $F_D(t,\xi)$.

Notions on UQ

Drag control - A few results

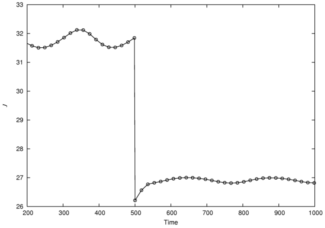

Temporal evolution of the cost function (-15%). The control is applied at $t = 500$.

Suction:

- $\longrightarrow$ narrows the cylinder wake,
- $\longrightarrow$ postpones the boundary layers separation.

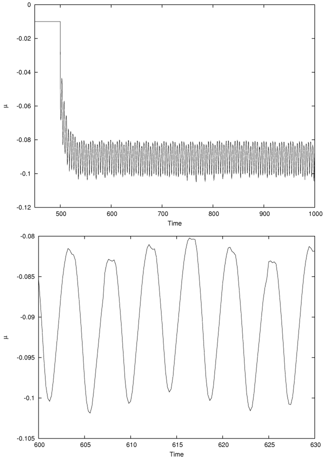

Optimal distribution of the control intensity $\mu(t)$.

Control characterization

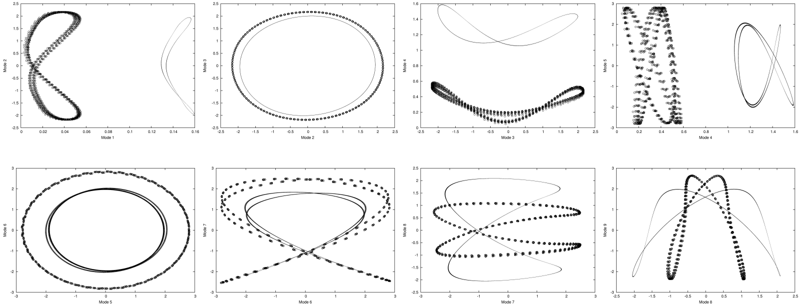

Phase portraits evolution with control. Circles: non-controlled flow; solid line: controlled flow.

$\Longrightarrow$ **Strong impact of the control.**

Control performance

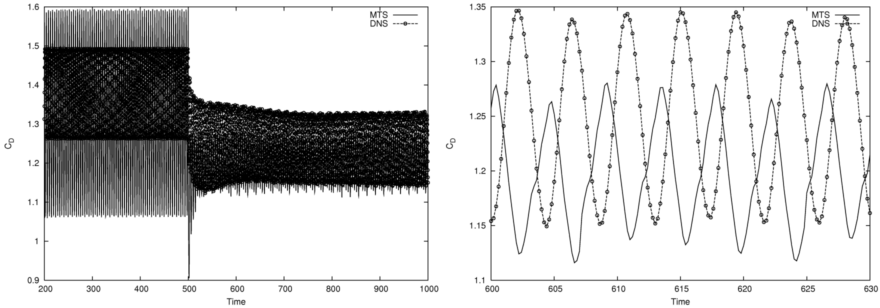

Drag time-evolution.

$\Longrightarrow$ Reduction by 11 % of the total drag ($\overline{C_D}$ = 1.38 $\longrightarrow$ 1.23)
depends on α, β (and γ)
$\Longrightarrow$ Control relevant for actual flows (validated by DNS)

Performance of the robust approach

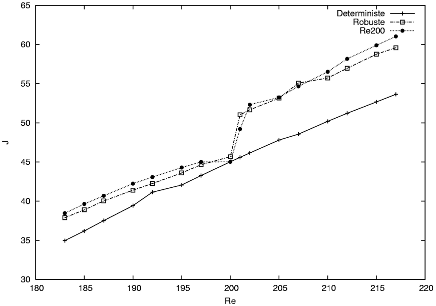

Performance of the different control strategies.

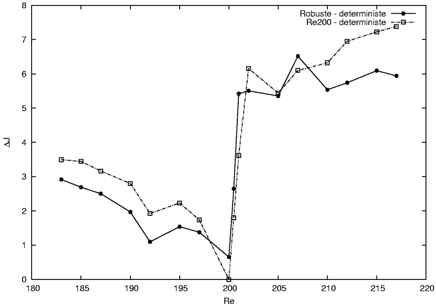

$\Delta\mathscr{J}$ between robust and non-robust (deterministic) control.

$\Longrightarrow$ **The control is robust.**

Application to a “real” flow

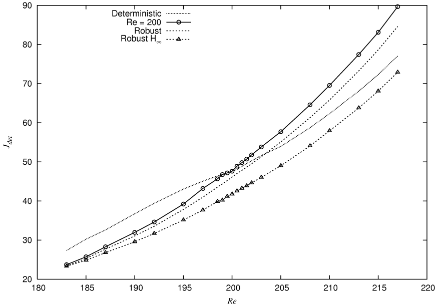

Cost function for different *Re*.

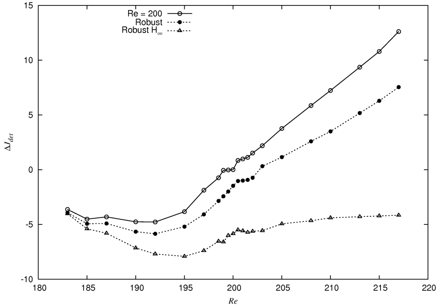

$\mathscr{J}$ gap between robust and deterministic control (DNS).

$\Longrightarrow$ Considering robustness of the control is all the more necessary as it is based on a reduced model !

The model reduction is here similar to a perturbation from the control performance point of view.

Part II: Optimal reduction for experiments

Optimal reduction for subsequent use in experiments

One wants the ROM:

- to accurately reproduce the action of the actuator (controllability),
- to be optimal w.r.t. the objective function to control (say cylinder drag F_D).

It is further desirable the basis be orthonormal. It leads to:

$$u^h(t, \boldsymbol{x}) = \sum_i a_i(t)\, \phi_i(\boldsymbol{x}), \qquad \mathscr{J} = \left\langle \left(F_D(t, \mu, Re) - F_D^h(\boldsymbol{a}, \mu, Re) \right)^2 \right\rangle_{\Omega_t \otimes \Omega_\mu}$$

with the desirable properties:

- orthogonality, $\left(\phi_i(\boldsymbol{x}); \phi_j(\boldsymbol{x})\right) = \delta_{ij}\ \left(\phi_i(\boldsymbol{x}); \phi_i(\boldsymbol{x})\right)$,
- normality, $\left(\phi_i(\boldsymbol{x}); \phi_i(\boldsymbol{x})\right) = 1$.

and the constraint: $a_i(t) = \left(u(t, \boldsymbol{x}); \phi_i(\boldsymbol{x})\right)$.

The ROM is supposed to belong to the subspace spanned by the primal snapshots (from a dirac impulsion of the actuators): $\phi_i(\boldsymbol{x}) = \sum_j \gamma_j\, u_p(\boldsymbol{x})$.

Further, in a closed-loop context, one may want the ROM to be observable.

Optimal reduction for subsequent use in experiments (cont'd)

$$
\begin{aligned}
\mathscr{L} \quad = \quad & \left\langle \left(F_D(t,\mu,Re) - F_D^h(\boldsymbol{a},\mu,Re) \right)^2 \right\rangle + \left\langle \beta_1 \sum_{i,j>i} \left(\phi_i(\boldsymbol{x}); \phi_j(\boldsymbol{x}) \right) \right\rangle \\
& + \left\langle \beta_2 \sum_i \left(1 - \left(\phi_i(\boldsymbol{x}); \phi_i(\boldsymbol{x})\right)\right)^2 \right\rangle - \beta_3 \,\mathrm{Tr}\left(Y^* \Phi \right) + \sum_i \langle \lambda_i \ \left(a_i(t) - \left(u(t,\boldsymbol{x}); \phi_i(\boldsymbol{x}) \right) \right) \rangle
\end{aligned}
$$

This is an optimization problem.
Solved using a l-BFGS algorithm. Efficient and cheap as the process only deals with the ROM.

Solution method:

1. solve the state and adjoint equations,
2. compute the Lagrangian gradient and evaluate the cost function $\mathscr{J}$,
3. update γs according to the Lagrangian gradient,
4. compute the new basis vectors ϕ_i and come back to step 1 until convergence.

Primal and adjoint snapshot

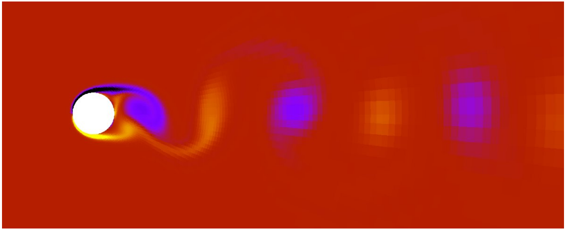

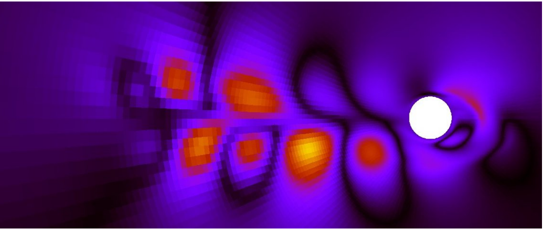

Objective functions

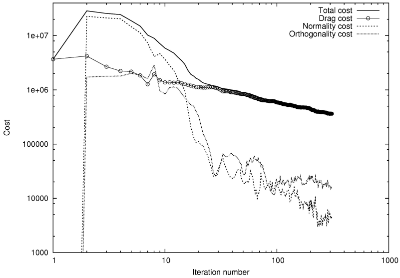

Objective function for optimal basis.

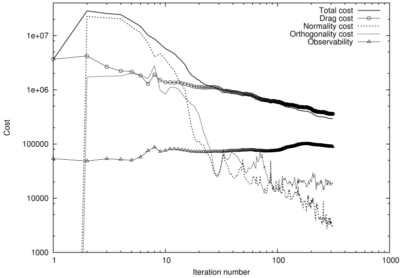

Objective function for optimal and observable basis.

Effect of the inclusion of the observability criterion on the basis performance.

Optimal basis modes

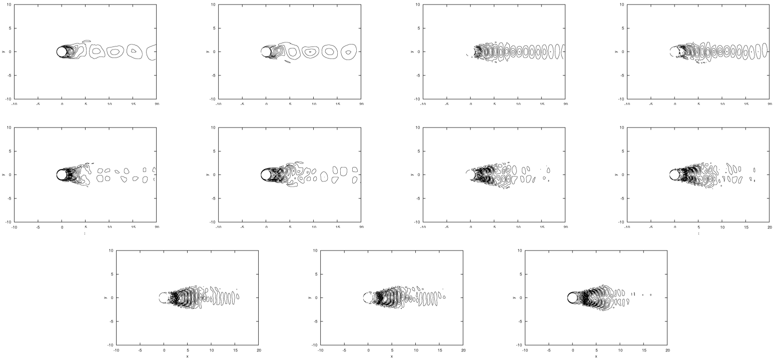

Optimal ROM modes 1 to 11.

Observable optimal basis modes

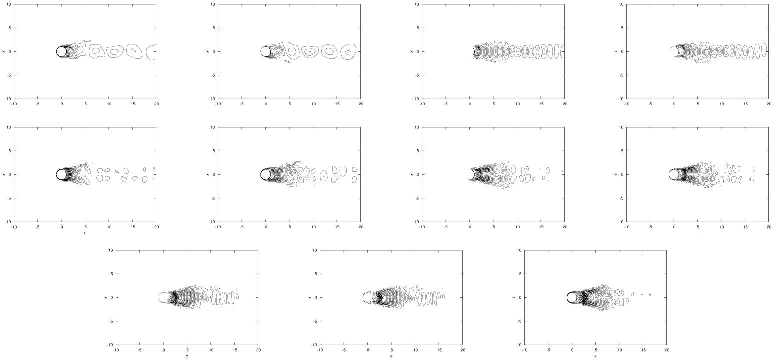

Observable optimal ROM modes 1 to 11.

As a conclusion...

Three ingredients of the recipe have been investigated:

- a robust reduced model of the original system which was proved both robust and accurate,
- a cheap and accurate time marching scheme,
- a $\mathscr{H}_\infty$-formulation of the objective function allowing for a robust control while maintaining good performances.

Derivation of a ROM suitable for experimental setup and closed-loop control was skimmed though more work is necessary.

Perspectives:

- improve the model robustness (robust balanced POD, $\mathscr{H}_\infty$ basis, ...),
- guarantee an upper bound for the probability of "undershoot" below a certain level of performance,
- development of techniques allowing to deal with large scale problems with a larger number of independent random variables,
- preliminary work on invariant subspace optimal reduction.

As a conclusion...

Three ingredients of the recipe have been investigated:

- a robust reduced model of the original system which was proved both robust and accurate,
- a cheap and accurate time marching scheme,
- a $\mathscr{H}_\infty$-formulation of the objective function allowing for a robust control while maintaining good performances.

Derivation of a ROM suitable for experimental setup and closed-loop control was skimmed though more work is necessary.

Perspectives:

- improve the model robustness (robust balanced POD, $\mathscr{H}_\infty$ basis, ...),
- guarantee an upper bound for the probability of “undershoot” below a certain level of performance,
- development of techniques allowing to deal with large scale problems with a larger number of independent random variables,
- preliminary work on invariant subspace optimal reduction.

Notions on uncertainty quantification

One needs to be able to quantify the uncertainty in the drag.

Several techniques:

- MonteCarlo and variants. Simple but potentially extremely costly (DNS. . .),
- FORM/SORM. Limited to low variance systems,
- Neumann series decomposition. Complex, or even impossible, in the general case,
- Polynomial Chaos. None of these drawbacks ?

Notions on the Polynomial Chaos

Parameterization of the data: $D = D(\theta) = D(\xi(\theta))$ with θ an elementary event of the probability space $(\Theta, \mathcal{B}, dP)$.

Spectral decomposition of a random variable:

$$U(x,t,\xi) = \sum_{j=0}^{P} u_j(x,t)\, \Psi_j(\xi(\theta)), \qquad \xi \in \Omega_\xi \subset \mathbb{R}^n,$$

with

$$\begin{aligned} \langle \Psi_k \Psi_l \rangle_{\Omega_\xi} &= \int_{\Omega_\xi} \Psi_k(\xi)\, \Psi_l(\xi)\, p_\xi(\xi)\, d\xi = \delta_{kl} \left\langle \Psi_k^2 \right\rangle_{\Omega_\xi}, \\ P+1 &= \frac{(n+p)!}{n!\, p!}. \end{aligned}$$

Two major formulations for PC

Let the physical model:

$$\mathcal{M}(S(\theta), D(\theta)) = 0, \qquad \forall \theta \in \Theta.$$

Solving by Galerkin projection...

$$\langle \Psi_k; \mathcal{M}(S(\theta), D(\theta)) \rangle = 0, \qquad \forall k = 1, 2, \ldots$$

...or by non intrusive formulation using quadrature / cubature:

$$S_k = \langle S(\xi(\theta)); \Psi_k(\xi(\theta)) \rangle \,, \qquad \forall k = 1, 2, \ldots$$

Back to the control

Sparse grid integration

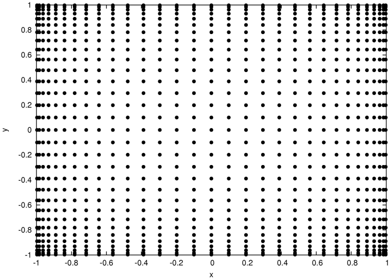

Gauss-Legendre quadrature: 961 points.

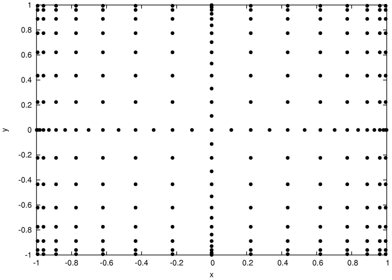

Smolyak scheme: 257 points.

Comparison of tensorized and regular sparse integration (2-D).

We are using adapative sparse grid $\longrightarrow$ even less number of points to consider. Back to the robust POD